



SPATIAL CORRELATION STUDY ON EARTHQUAKE GROUND MOTION BASED ON ARRAY DATA

Turgay TÜRKER

*Graduate Student
Institute of Industrial Science
The University of Tokyo
7-22-1 Roppongi, Minato-ku
Tokyo 106, JAPAN*

Fumio YAMAZAKI

*Associate Professor
ditto*

Tsuneo KATAYAMA

*Professor
ditto*

SUMMARY

A frequency-wavenumber spectrum model has been used in order to demonstrate the spatial correlation characteristics of earthquake ground motion. The proposed model is considered as a non-quadrant symmetric with respect to the wavenumber axes k_x and k_y . Then, spatial variability and correlation analyses are made for uni-directionally propagating earthquake ground motion depending upon the apparent velocity and the azimuthal angle.

By selecting the 1985 Ibaragiken-Nanbu earthquake from the Chiba array database, the space-time cross spectral density function is computed from the model to reveal the spatial correlation characteristics of this event.

The spatial coherence of this event is also computed as a function of spatial distance and frequency. The computed spatial coherence functions are compared with those from the observed data.

1. INTRODUCTION

Ground motion observed during strong earthquakes may vary both in time and space, and is a composite of seismic waves with various characteristics. Hence, no simple relationship can be assigned to the frequency and wavenumber.

Seismic array data, supplying essential knowledge about the spatio-temporal variations of seismic ground motions, have been studied by a number of researches. Then coherence models were proposed which can be used in the design of spatially extended engineering structures such as pipelines, tunnels,

bridges etc. Using the SMART-1 array data, several authors have studied the coherence relation. The proposed coherency models [1], [2], [3] are dependent on the distance between two stations and frequency. Hao et. al. [4] developed a model in which coherency is dependent on both projected distance along the direction of wave propagation and that transverse to it.

As an alternative, the frequency-wavenumber spectra can be studied since these effectively describe the temporal and spatial variability of seismic ground motion. FK spectra also provide information about spatial correlation characteristics of earthquake ground motion. A lot of papers were published for this purpose such as [5], [6], [7], [8] etc.

The frequency-wavenumber (FK) spectrum model proposed by Yamazaki and Türker [9] was employed for the Ibaragiken-Nanbu earthquake to demonstrate the space-time correlation structure during the wave propagation.

2. THE CHIBA SEISMOMETER ARRAY

The Chiba Experiment Station is located about 30 km east of Tokyo. Installation of three-dimensional (3D) Chiba array was completed in April 1982. Figure 1 shows the configuration of boreholes in the Chiba array. The eight boreholes are very densely located around the C0 borehole (in 30m x 30m area). The four boreholes (C1-C4) are in the distance of 5m from the C0 borehole and the other four (P1-P4) are 15m away from the C0. The borehole accelerometers are installed at five different depths, GL-1m, -5m, -10m, -20m and -40m.

Figure 2 illustrates a histogram of the separation distances for all of the borehole pairs. The topography is very flat with elevations ranging between 10.92m and 13.65m above the sea level across the array.

Approximately 160 earthquake events were recorded since 1982. During construction of the Chiba array database, 27 major earthquakes were selected. The detailed information on this database has been given in [10].

The Ibaragiken-Nanbu earthquake (Event 8519) occurred on October 4, 1985 was selected from the database in order to demonstrate the spatial correlational characteristics due to body waves. The epicentral distance was 28km with a direction of N9°E. The magnitude of the event was 6.1 in the JMA scale with a focal depth of 78km. This event is the second strongest earthquake in the database.

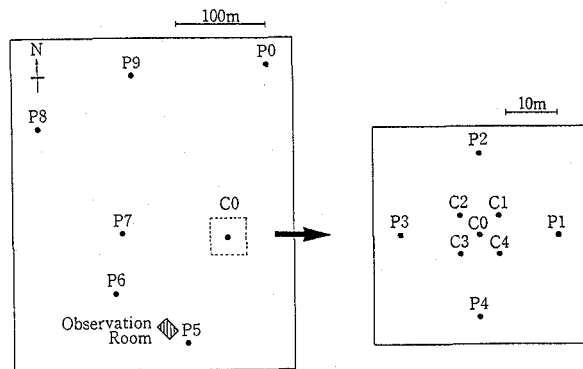


Fig. 1 Borehole Configuration of Chiba Array at Ground Surface

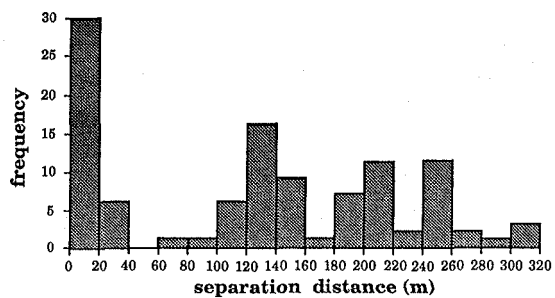


Fig. 2 Histogram of Separation Distance between Borehole Pairs in Chiba Array

The EW- and NS-components of the acceleration record obtained at fifteen boreholes at GL-1m, shown in Fig. 3, were used in this study.

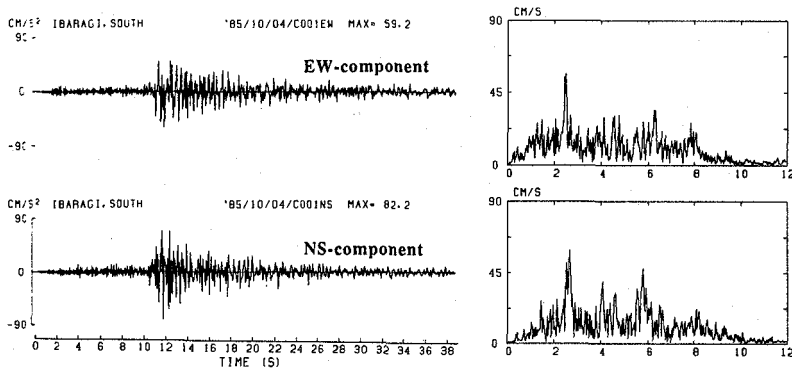


Fig. 3 Time Histories and Their Fourier Spectra of Ibaragiken-Nanbu Earthquake for EW- and NS- Components at C001 (C0 Borehole at GL-1m)

3. FREQUENCY-WAVENUMBER SPECTRUM MODEL

Assuming that a space-time process $u(x, y, t)$ is stationary in time, homogeneous in space and ergodic in both, the following three-dimensional FK spectral density function is used.

$$S(k_x, k_y, f) = G(f) A(k_x, k_y | f) \quad (1)$$

where $G(f)$ is the one-sided power spectral density function, and $A(k_x, k_y | f)$ is the normalized conditional wavenumber spectrum at frequency f . For this two-dimensional wavenumber spectrum, the following anisotropic exponential function is considered.

$$A(k_x, k_y | f=f_i) = B_i(k_x, k_y) = \frac{\alpha_x \alpha_y}{\pi} \exp[-(\alpha_x k_x')^2 - (\alpha_y k_y')^2] \quad (2)$$

where α_x and α_y are parameters with the dimension of length and are expressed as functions of frequency. These parameters control the shape of the wavenumber spectrum at each frequency and the following functional forms are considered.

$$\alpha_x(f) = a_1 \exp(-f^{a_2 + a_3 f}); \quad \alpha_y(f) = b_1 \exp(-f^{b_2 + b_3 f}) \quad (3)$$

The new wavenumber coordinates, k_x' and k_y' , can be obtained by a two-dimensional coordinate transform shown in Fig. 4. For a fixed frequency, this model possesses an ellipsoidal correlation structure in wavenumber field. If dominant apparent velocity c and azimuthal angle θ are given, the corresponding peak location of the FK spectrum model is obtained by $k_{x0} = (f \sin\theta) / c$ and $k_{y0} = (f \cos\theta) / c$.

4. BRIEF SUMMARY OF SPACE-TIME CORRELATION STRUCTURE

Frequency-wavenumber spectrum $S(\mathbf{k}, f)$ and space-time cross spectral density function $C(\xi, f)$ have the following two-fold Wiener Khintchine transform pair:

$$C(\xi, f) = \int_{-\infty}^{\infty} S(\mathbf{k}, f) e^{i \xi \cdot \mathbf{k}} d\mathbf{k} \quad (4)$$

$$S(\mathbf{k}, f) = \left(\frac{1}{2\pi}\right)^2 \int_{-\infty}^{\infty} C(\xi, f) e^{-i \xi \cdot \mathbf{k}} d\xi \quad (5)$$

where $\mathbf{k} = (k_x, k_y)^T$ and $\xi = (\xi_x, \xi_y)^T$ are the wavenumber vector and the separation vector, respectively.

The space-time cross spectral density function, $C(\xi, f)$ is complex when non-quadrant symmetry is considered with respect to wavenumber axes k_x and k_y in the FK spectrum, $S(\mathbf{k}, f)$.

Thus, the spatial coherence function $|\rho_f(\xi)|^2$ is computed as

$$|\rho_f(\xi)|^2 = \frac{|C(\xi, f)|^2}{S^2(f)} \quad (6)$$

When $\xi=0$ is taken in Eq. 4, the power spectral density function $S(f)$ in Eq. 6 becomes:

$$C(0, f) \equiv S(f) = \int_{-\infty}^{\infty} S(\mathbf{k}, f) d\mathbf{k} \quad (7)$$

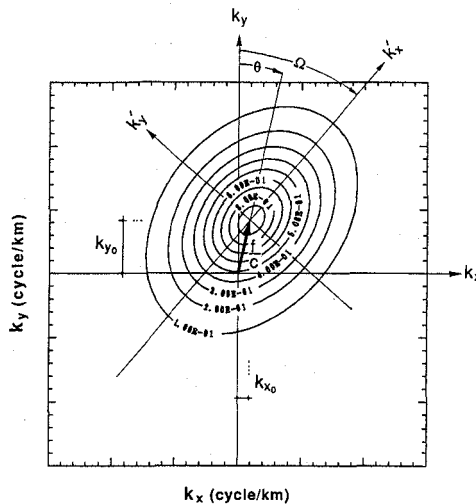


Fig. 4 Transformation of Wavenumber Coordinates

5. SPATIAL CORRELATION ANALYSIS

5.1 Directionality Analysis for the Ibaragiken-Nanbu Earthquake

For the Ibaragiken-Nanbu earthquake, an analysis is made in order to reveal the direction dependency of the parameters which governs the wave propagation such as apparent velocity, azimuthal angle, etc. The EW- and NS-components of this event, at GL-1m for $t=11-21$ s time segment which correspond to the S-wave part, are selected for fifteen station points. Then, the EW- and NS-components are rotated into six directions with 30° increments, Fig. 5. Then, FK spectrum analysis is conducted to obtain the variation in the apparent velocity and the azimuthal angles with frequency for the six different directions. This analysis is made for center frequencies between 0.39Hz and 8Hz with an approximately 0.1Hz interval. The results are shown in Figs. 6 and 7.

The apparent velocity and azimuthal angle show rather constant values for the frequency range less than 5Hz, and their fluctuating parts mostly correspond to frequency contents with small power. The azimuthal angles evaluated by the observed data for the six direction were mostly close to the direction of the epicenter. The apparent velocity was in the range of 4-6 km/s for most frequencies in the all directions, while the shear wave velocity of the top soil layer is 140 m/s according to geophysical exploration. Hence, the incident angle of the seismic waves is found to be almost vertical to the ground surface.

By integrating the wavenumber power spectra over the wavenumber axes, the power spectra for the six direction can be obtained as shown in Fig. 8. The power spectra obtained for the six directions showed almost similar spectral amplitudes.

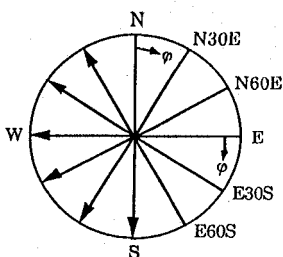


Fig. 5 Six Different Directions

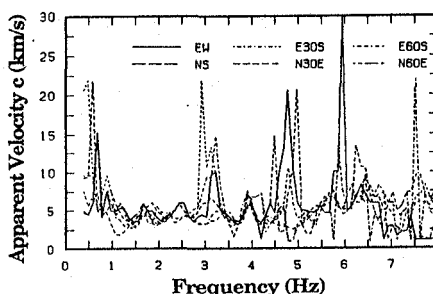


Fig. 6 Variation of Apparent Velocity for Six Directions

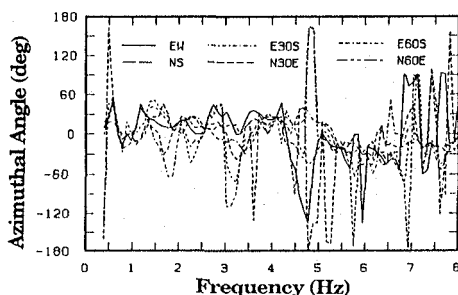


Fig. 7 Variation of Azimuthal Angle for Six Directions

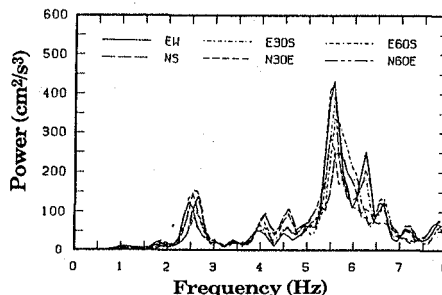


Fig. 8 Power Spectra for Six Directions (by integration of FK spectra)

5.2. Space-Time Cross Spectral Density Function

From the directionality analysis in the previous section, homogeneity of the ground motion may be assumed. Assuming that earthquake ground motion is homogeneous, a three-dimensional FK spectrum model is constructed according to Eqs. 1-3 by selecting the EW-component for time segment for $t=11-21s$ at fifteen station points. The power spectrum $G(f)$ in Eq. 1 is also modeled as a superposition of three Gaussian function for the center frequencies of 2.44Hz, 5.57Hz and 6.25Hz with the amplitudes and shapes being consistent with the observed one in Fig. 8 (EW-component). When constructing the model, the apparent velocity and azimuthal angle are assumed as $c=4.0km/s$ and $\theta=9^\circ$, respectively. Then, $C(\xi, f)$ is computed according to Eq. 4 using the analytical 3D FK spectrum model.

Figure 9 shows the real and imaginary parts of $C(\xi, f)$ in space coordinates at three frequencies. The target azimuthal direction of $\theta=9^\circ$ is seen in both the real and imaginary parts of $C(\xi, f)$. Since there is an inverse relationship between the wavenumber coordinates and the space coordinates, the wave length of the propagation ($L_w = 1/k = c/f$) can be clearly observed in the imaginary part of $C(\xi, f)$. The dominant wave length of the propagation is measured between two zero contour lines on the azimuthal direction as shown in Fig. 9.

In the case of a quadrant symmetric FK spectrum model, the imaginary part of the $C(\xi, f)$ would be zero because of the evenness of the FK spectrum with respect to the wavenumber axes k_x and k_y .

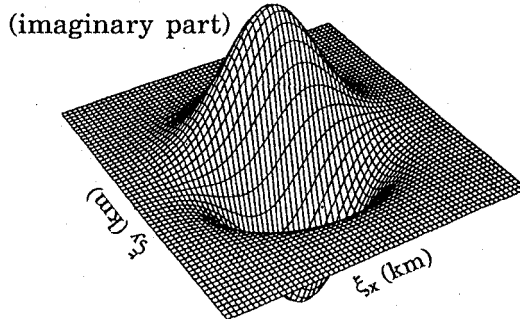
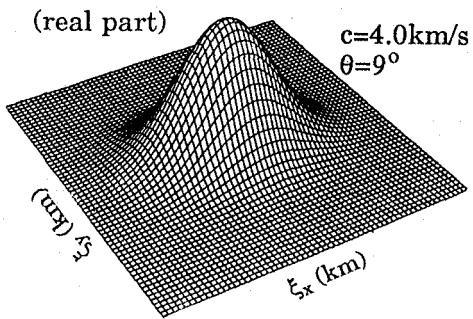
5.3. Spatial Coherence Function Obtained from the FK Model

Using Eqs. 6-7, the spatial coherence functions were computed and illustrated for six frequencies in Fig. 10. From this figure, larger coherence is observed in the normal to the azimuthal direction θ . The loss of coherence with separation distances ξ_x and ξ_y , can also be clearly seen. A section of 3D spatial coherence function was plotted as a function of frequency for fixed separation distances in Fig. 11.

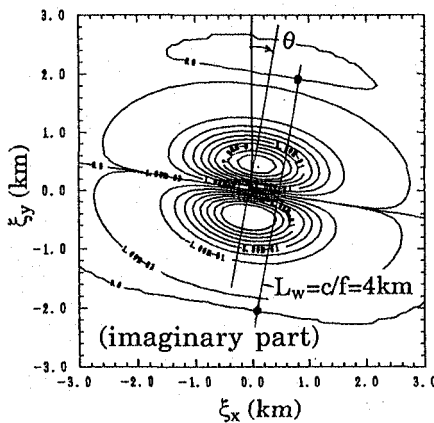
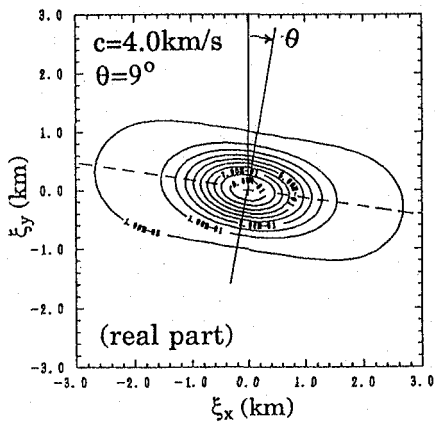
Figure 12 compares the coherence functions obtained by the above procedure and by the ordinary two-point coherence calculation which was performed for the radial- and transverse components of the observed data. The Parzen window was used (bandwidth=0.4Hz) in two-point coherence calculations.

In Fig. 12a, the separation distance was so short ($\xi=5.7m$) that all coherences were found to be close to 1.0 between 0 and 8Hz. The model gave almost unit coherence in all frequencies. A good agreement between the coherences given by the model and the observed coherences is seen in Figs. 12b-12c. In Fig. 12d, the analytically obtained coherences were found to be slightly lower than the observed ones. The rapid decrease in frequency is seen for separation distances longer than approximately 250m because there were few separation distances exceeding this value. This can be due to the dense array configuration. However, the maximum separation distance, between the stations P5 and P0, is 319.2m, therefore, it was difficult to have good coherence functions for the separation distances longer than this value.

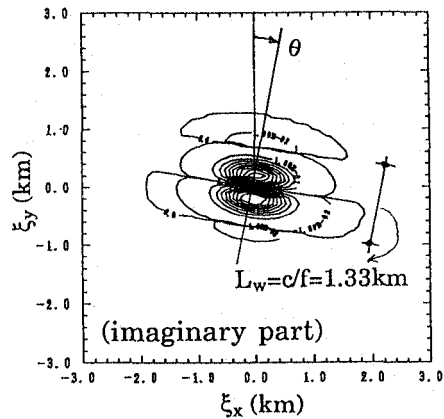
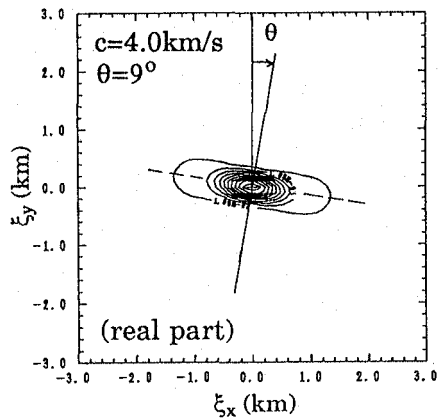
Generally, the decrease of the modeled coherence functions with frequency was found to be lower than the observed ones for short separation distances. In contrast, the decrease of the modeled coherence with frequency was found to be higher than the observed ones for longer separation distances due to the Gaussian form of the coherence structure.



a) at $f=0.5\text{Hz}$

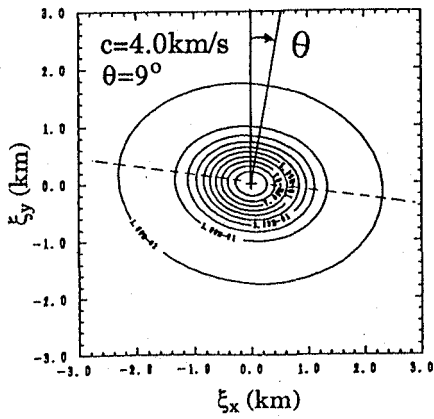


b) at $f=1.0\text{Hz}$

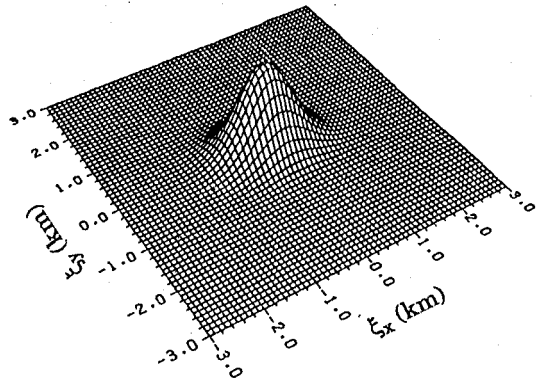


c) at $f=3.0\text{ Hz}$

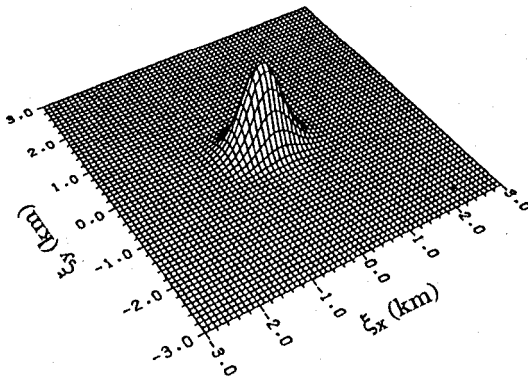
Fig. 9 Space-Time Cross Spectral Density Function



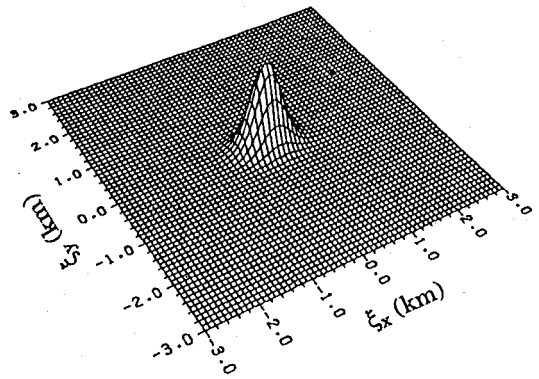
a) at $f=0.5 \text{ Hz}$



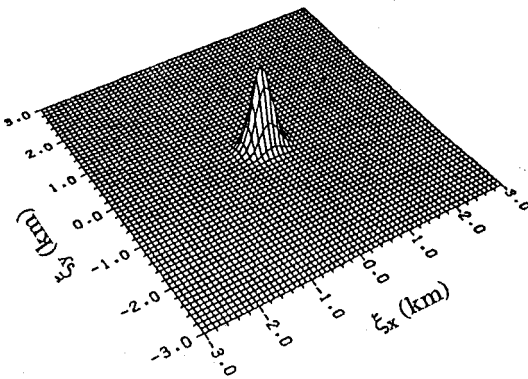
b) at $f=1.0 \text{ Hz}$



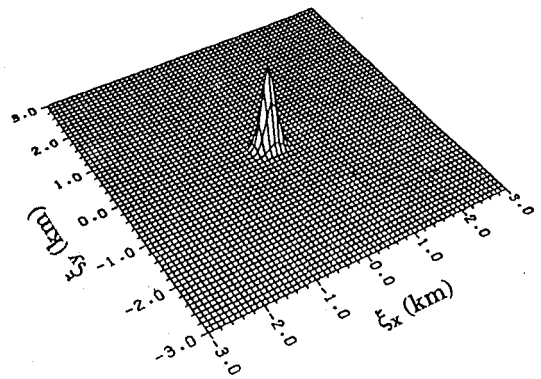
c) at $f=2.0 \text{ Hz}$



d) at $f=3.0 \text{ Hz}$

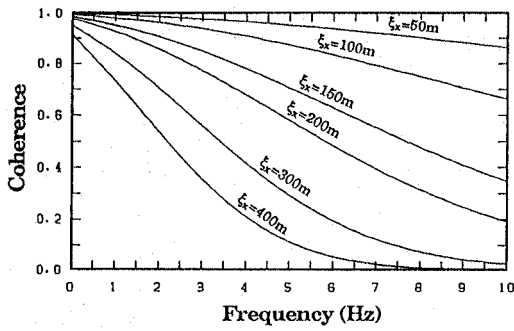


e) at $f=5.0 \text{ Hz}$

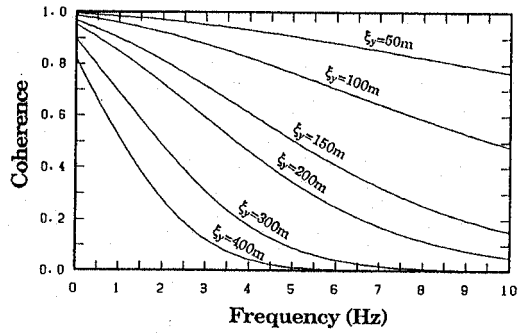


f) at $f=8.0 \text{ Hz}$

Fig. 10 Spatial Coherence Function



a) separation distance ξ_x ($\xi_y=0$)



b) separation distance ξ_y ($\xi_x=0$)

Fig. 11 Spatial Coherence Functions for Fixed Separation Distances

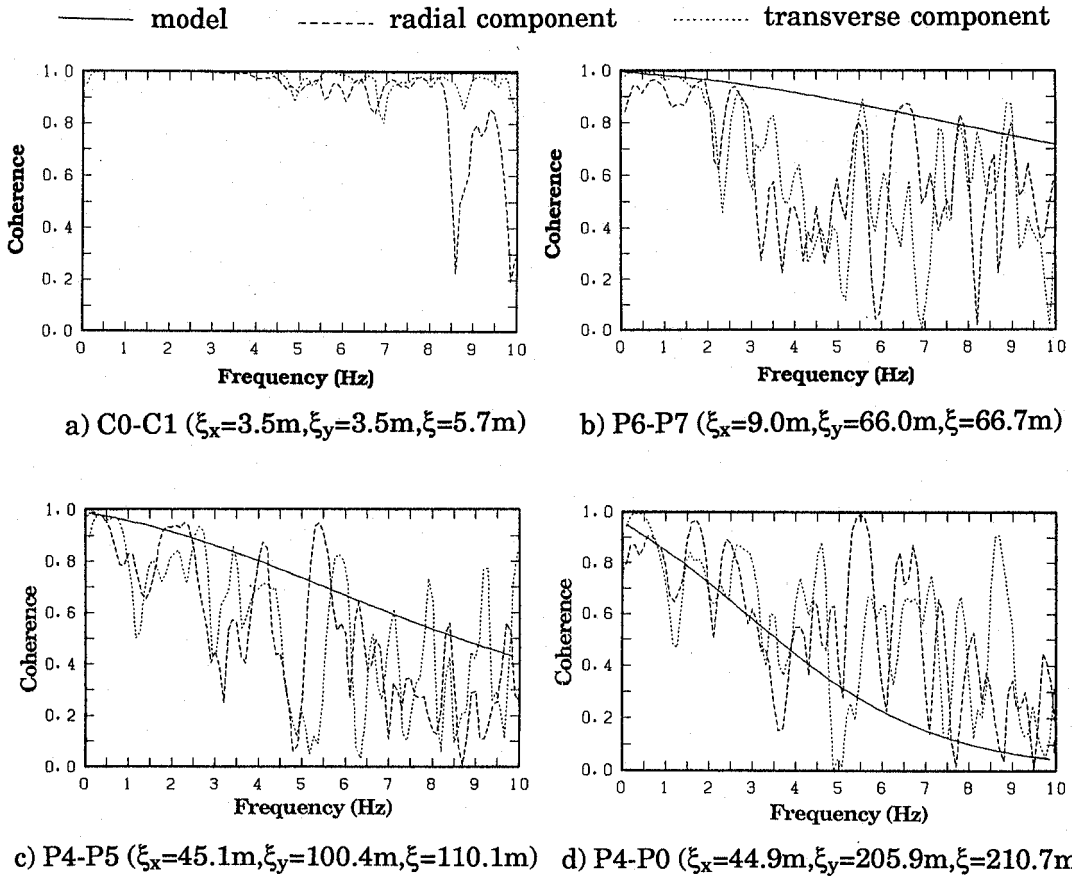


Fig. 12 Comparison of Coherence Functions for Four Station Pairs
(between our model and the observed radial- and transverse-components)

6. CONCLUSIONS

The frequency-wavenumber spectrum model was constructed by using the records of the Ibaragiken-Nanbu earthquake. Then, the space-time cross spectral density function was computed by taking the double inverse Fourier transform of the model with respect to the wavenumber axes. The real and imaginary parts of the space-time cross spectral density function showed a clear consistency with the azimuthal direction and the apparent wave velocity of this event.

The spatial coherence functions were derived with the aid of the FK spectrum model. The analytically obtained spatial coherence functions were compared with the observed ones for several separation distances. A rapid decrease of coherence with frequency was observed for increasing separation distances due to the Gaussian form of the coherence structure. Since FK spectrum analysis usually reveals the signal parts of propagating seismic waves, it is natural to see some discrepancies between the observed and modeled coherences. When noise coherences are suppressed by averaging the observed coherences, it is believed that a better agreement may be found than those presented here. It was also concluded that the applicability of coherence models using seismic array data is limited with the maximum separation distance between the station points. It is worthwhile to do similar analysis for different array records.

REFERENCES

- [1] Loh, C. H., Analysis of the Spatial Variation of Seismic Waves and Ground Movements from SMART-1 Array Data, J. EESD, Vol. 13, pp. 561-581, (1985).
- [2] Harichandran, R. S. and Vanmarcke, E. H., Stochastic Variation of Earthquake Ground Motion in Space and Time, J. Engrg. Mech., ASCE, Vol. 112, No. 2, pp. 154-174, (1986).
- [3] Kataoka, N., Morishita, H. and Mita, A., Spatial Variation of Seismic Ground Motion at Lotung Soil-Structure Interaction Experiment Site, Proc. of the 8th Japan Earthquake Engineering Symposium, Vol. 1, pp. 607-612, (1990).
- [4] Hao, H., Oliveira, C. S. and Penzien, J., Multiple-Station Ground Motion Processing and Simulation Based on Smart-1 Array Data, Nuclear Engrg. and Design, No:111, pp. 293-310, North-Holland, Amsterdam, (1989).
- [5] Abrahamson, N. A., Estimation of Seismic Wave Coherency and Rupture Velocity Using the SMART1 Strong-Motion Array Recordings, EERC Report 85/02, University of California, Berkeley, CA, (1985).
- [6] Deodatis, G., Shinozuka, M. and Papageorgiou, A., Frequency-Wave Number Spectra from Seismic Sources in a Half-Space, Proc. of 4th U.S. National Conference on Earthquake Engineering, Vol. 1, pp. 447-456, (1990).
- [7] Deodatis, G., Shinozuka, M. and Papageorgiou, A., Stochastic Wave Representation of Seismic Ground Motion. I: FK-Spectra, J. Engrg. Mech., ASCE, Vol. 116, pp. 2363-2379, (1990).
- [8] Türker, T., Yamazaki, F. and Katayama, T., Simulation of Earthquake Ground Motion Based on Frequency-Wavenumber Spectrum, Transactions of the 11th International SMiRT Conference, (1991).
- [9] Yamazaki, F. and Türker, T., Stochastic Modeling of Earthquake Ground Motion Based on Chiba Array Records, Proc. of ICASP 6, (1991).
- [10] Katayama, T., Yamazaki, F., Nagata, S., Lu, L. and Türker, T., A Strong Motion Database for the Chiba Seismometer Array and its Engineering Analysis, J. EESD, Vol. 19, pp. 1089-1106, (1990).